

Diffracted Beam–Transmitted Beam Borrmann X-ray Topography in Copper. A Novel Method of Stereo Depth Topography

BY G. P. HAMILL* AND T. VREELAND JR

W. M. Keck Laboratory of Engineering Materials, California Institute of Technology, Pasadena, California 91125, USA

(Received 28 July 1978; accepted 12 February 1979)

Abstract

The observed depths of dislocations, as measured from the exit surface of a copper single crystal, are within a region of the crystal where μd , the kinematic linear absorption coefficient times the depth, is less than or approximately equal to unity. Splitting of the Borrmann wave into its diffracted and transmitted beam components is indicated in relatively perfect portions of the crystal near the exit surface.

Introduction

Direct observations of the three-dimensional geometry of dislocations using non-destructive procedures is a valuable tool in the study of the microscopic stress-strain properties of a crystalline material. The present investigation was undertaken to extend Vreeland's work on zinc (Vreeland, 1976) to copper and to provide quantitative depth measurements of dislocations in single crystals of high-purity copper using Borrmann transmission topography.

The depth of dislocations below the specimen surface may be determined from stereo pairs of X-ray transmission topographs which are taken using one of two methods; the first proposed by Lang (1958, 1959*a, b*), and the second by Haruta (1965). Lang proposed using a pair of topographs, of the reflections hkl and $\bar{h}l\bar{k}$, which provides a stereo viewing angle of $2\theta_B$, where θ_B is the Bragg angle for the reflection. This method is convenient for thin specimens in which one can obtain Lang transmission intensities of reasonable magnitude. By using the same set of reflecting planes but rotating about the normal to the reflecting planes between topographs, one obtains with Haruta's method a pair of asymmetrical stereo topographs with an adjustable stereo angle. Haruta's method can be used in both Lang and Borrmann transmission topography.

Narasimhan & Roessler (1975, 1976) applied Haruta's method to Borrmann transmission topography by placing a film in direct contact with the exit surface of the crystal for each of the asymmetric topographs. The adjustable stereo angle between topographs, coupled with the increased intensity (summing

of the $K\alpha_1$ and $K\alpha_2$ diffracted beams and the transmitted beam) and the undistorted topograph 'map' of the image of the crystal, gives this method a strong advantage over other topographic methods. However, the disadvantage of having to make contact between the film and the surface of a highly-perfect soft crystal cannot be ignored.

If it is assumed that all the beam energy in Borrmann transmission is carried to the exit surface along the diffracting planes, no stereo information should be available from the hkl and $\bar{h}k\bar{l}$ pair of diffractions. Similarly, no stereo information should be available from the diffracted and transmitted beams obtained separately and simultaneously under one set of diffraction conditions.

In all Borrmann topography, the Bloch wave established in the crystal is a standing wave transmitted through the crystal along the diffracting planes (Borrmann, 1941; Azaroff *et al.*, 1974; for a more complete reference list and review see Tanner, 1976). In an otherwise nearly perfect crystal, if a region exists in which a localized strain field causes the diffracting planes to be distorted, this region will decouple the Bloch wave into its respective diffracted and transmitted beam components. Such is the case near a dislocation and near the free surfaces of the crystal. A dislocation deep within a crystal decouples the Bloch wave and each of the components is absorbed kinematically by the surrounding crystal. The information on this occurrence (a loss of intensity in the Bloch wave) is carried through the crystal along the diffracting planes to the exit surface. Near the exit surface, the free surface itself causes a relaxation and provides a means of decoupling the Bloch wave (Tanner, 1973).

The present work describes a study of diffracted beam and transmitted beam topographs, obtained separately but simultaneously with the film placed parallel to the exit surface of the crystal. Stereo depths of the images of dislocations were observed. A corresponding set of stereo topographs using Haruta's method was also obtained and analyzed.

Experimental method

A cylindrical disc of high-purity copper single crystal, 11 mm in diameter and approximately 270 μm thick, oriented with its axis parallel to $[111]$, was machined

* Present address: Geological Science Department, McGill University, Montreal, Quebec H3A 2A7, Canada.

with a South Bay Technology Model 452 electrolytic lathing machine and a Model 451 electrolytic lapping machine. The polished surface was then scratched with quartz whiskers along the three $\langle 1\bar{1}0 \rangle$ directions lying in the (111) surface to ensure the presence of fresh dislocations near the surface of the crystal (Jassby & Vreeland, 1970). A square grid pattern of gold dots, with each dot approximately $0.5 \mu\text{m}$ thick by $40 \mu\text{m}$ in diameter, was vacuum evaporated onto the scratched surface to provide a depth reference.

The crystal was placed with the scratched surface as the exit surface for a Borrmann topograph on a double crystal system (Boettinger, Burdette, Kuriyama & Green, 1976). Characteristic Cu $K\alpha$ radiation was used for 220 diffraction (diffracting planes perpendicular to the crystal surface as in Fig. 1). The pair of Cu $K\alpha_1$ topographs, diffracted beam and transmitted beam, were obtained on a single Ilford L-4 plate ($50 \mu\text{m}$ thick emulsion) placed 15 mm from the exit surface of the crystal and parallel to the surface. Exposure time was 160 h.

The copper crystal was then removed from the double crystal system and placed in the direct beam from a narrow line-focus copper X-ray tube. Fig. 2 shows the geometrical conditions for the asymmetrical pair of stereo topographs obtained with Haruta's (1965) method and 220 diffracting planes. For the two topographs the crystal was rotated $\pm 10^\circ$ about $[1\bar{1}0]$ normal to the diffracting planes from the symmetrical position in which the incident and diffracted beams, the normal to the diffracting planes and the crystal surface normal are coplanar. The 'asymmetrical' diffracted beam topographs were also obtained on Ilford L-4 plates, which were placed approximately 10 mm from the exit surface of the crystal but skew to the surface to

avoid overlap of the transmitted beam image with the desired diffracted beam image. Exposure time was 40 h for each topograph. Enlarged negatives ($20\times$ magnification) of the topographs were made.

Stereo measurements on the pairs of magnified stereo topographs were made with a mirror stereoscope (Hilger and Watts, Model 5B-180 with binocular unit and 'flying spot' stereometer). The stereo shifts of the dislocations were measured with respect to the nearest gold dot images. Full stereo observations using both eyes simultaneously and a slightly modified blink system were used. The latter method, in which the observer alternately blinks his eyes to observe the images and the positions of the 'flying spot' on each topograph separately, proved more useful when the pair of topographs were of unequal intensity, when an observer found it impossible to accommodate the large stereo shifts easily, when the topographs were slightly distorted as in the pair of asymmetrical topographs, and in some cases where the gold dot reference points were imaged as described below.

Experimental results

A diffracted beam and transmitted beam stereo pair of 220 topographs is shown in Fig. 3. The corresponding asymmetrical pair of topographs is shown in Fig. 4. Both fresh dislocations introduced by the scratching and long straight grown-in dislocations are visible in the topographs. The long straight diffuse images are Cottrell-Lomer dislocations produced during the growth process (Kuriyama, Early & Burdette, 1974). The reference grid of gold dots is visible as light-dark spots in the diffracted beam topograph, and the contrast is reversed (dark-light) in the transmitted beam topograph of Fig. 3.

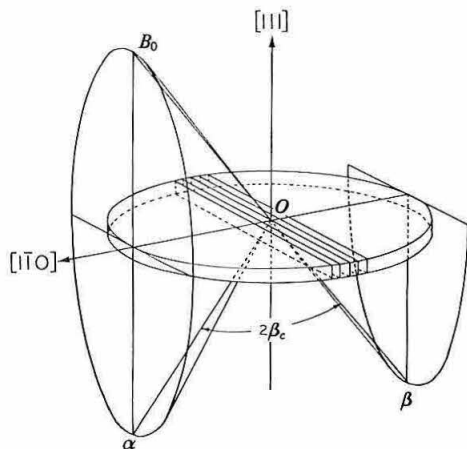


Fig. 1. Geometry for diffracted beam-transmitted beam Borrmann stereo topography from a (111)-oriented copper disk. The incident beam along B_0O of the Bragg cone is transmitted through the crystal by channelling along the $(1\bar{1}0)$ planes shown. The directions $O\alpha$ and $O\beta$ are, respectively, the diffracted and transmitted beam directions. $2\beta_c$ is the stereo angle, or, in this geometry, twice the Bragg angle, θ_B .

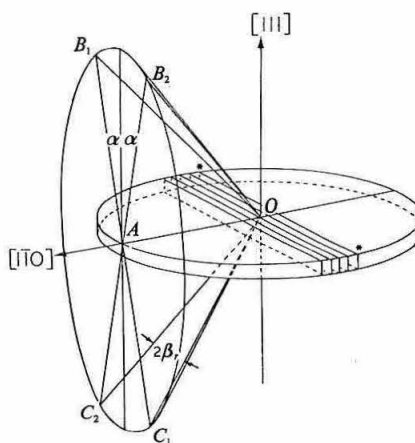


Fig. 2. Geometry for Borrmann stereo topography using Haruta's (1965) method. After rotating the crystal $\pm\alpha^\circ$ from the symmetric position, the two asymmetric topographs are taken with the X-ray paths being B_1OC_1 and B_2OC_2 . $2\beta_n$, the angle between the two diffracted beams, OC_1 and OC_2 , is the stereo angle. Stereo measurements are obtained in the $\star-\star$ direction along the diffracting planes.

Table 1. Apparent depth of dislocation images with respect to the images of the gold dots in Borrmann topography

Reflection used	Observed mean depth (μm)	Standard deviation (μm)	Minimum-maximum readings (μm)
Diffracted-transmitted beam $\bar{2}20$	-0.3	4.9	-7.6 to 10.6
Diffracted-transmitted beam $\bar{2}20$			
Cottrell-Lomer dislocations	3.4	4.6	-4.6 to 12.0
Asymmetric ($\pm 10^\circ$ from symmetric $\bar{2}20$ position)	152	75	3.5 to 264
Asymmetric ($\pm 10^\circ$ from symmetric $\bar{2}20$ position)			
Cottrell-Lomer dislocations	137	65	30 to 289

Note: Negative values of image depths denote images closer to the exit surface of the specimen than the images of the gold dots.

Dislocation images appear both above and below the gold dots in the stereo viewer for the diffracted-transmitted pair of topographs. This indicates that the image of the gold dot appears below the plane of the crystal surface (or that the images of the dislocations appear outside the crystal). The apparent depths of dislocation images, given in Table 1, fell between approximately $8 \mu\text{m}$ above the images of the gold dots to approximately $12 \mu\text{m}$ below in the diffracted-transmitted beam case, and from $3.5 \mu\text{m}$ to approximately $280 \mu\text{m}$ below the images of the gold dots in the asymmetric stereo pair using Haruta's (1965) method.

The range of dislocation depths observed did not vary significantly over the surface of the crystal. Thus, the observed depths were not the result of abnormalities in the grid deposition, nor the microscopic roughness of the surface, for example.

Gold dot image formation in Borrmann X-ray topography

Fig. 5 is a schematic drawing of a gold dot grown epitaxially on the surface of a specimen, the associated strain region within the copper crystal generated by the atomic mismatch of the two species, and the limiting

rays of radiation which produce the boundaries of its stereo image on the photographic plates for the diffracted and transmitted beam Borrmann topographs. The limiting ray geometry shows that the stereo image of the gold dot appears to be inside the specimen at a distance

$$H_0 = \frac{R_0(1 - \cos\theta_B)}{2 \sin\theta_B},$$

where θ_B is the Bragg angle for the reflection and R_0 is the radius of a hemispherical strain field within which the Borrmann Bloch wave is decoupled into the diffracted and transmitted beams. With $\theta_B = 37.06^\circ$ and R_0 approximately $20 \mu\text{m}$, the value for H_0 is $3.5 \mu\text{m}$ below the true surface of the crystal when one is measuring stereo depths by image shifts along the projected directions of the diffracted and transmitted beams.

The image of each gold dot was observed to have a light-dark pair of spots on the diffracted beam topograph and a corresponding dark-light image on the transmitted beam topograph. Superposition of the two images for each dot showed that there was very little absorption due to the gold dot (calculated absorption of $\text{Cu } K\alpha$ for $0.5 \mu\text{m}$ of gold is less than 3.5%), but that there was an energy transfer between the diffracted beam and the transmitted beam. Kuriyama (1969) and

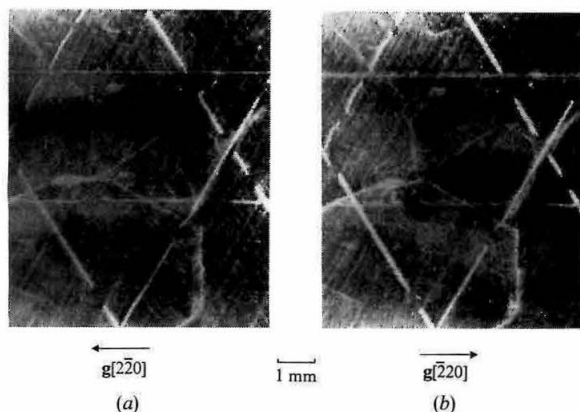


Fig. 3. Borrmann diffracted (a) and transmitted (b) beam stereo pair. The light-dark contrast of the images of the gold dots is visible, as well as individual dislocations and small angle boundaries. Some short and long scratches are also visible along the three $\langle 220 \rangle$ directions in the (111) plane of observation. The projections of the reflection vectors g are shown.

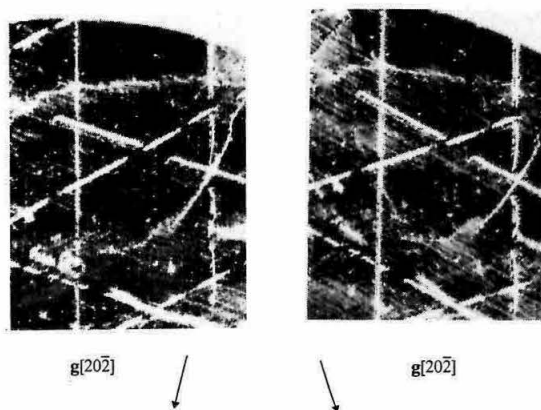


Fig. 4. Asymmetric Borrmann stereo topographs taken $\pm 10^\circ$ from the symmetric position. Note the large image shifts of the long dislocations, implying very deep observations. The projections of the reflection vectors g are also shown.

Tanner (1976) have both shown that the intensities for each beam can be written in this case as

$$I_{\text{diff}} = I_0 + I_1 \sinh(\mathbf{k} \cdot \mathbf{u}),$$

$$I_{\text{tran}} = I_0 - I_1 \sinh(\mathbf{k} \cdot \mathbf{u}),$$

where I_0 and I_1 are some calculable intensities, \mathbf{k} is the wave vector for the reflection, and \mathbf{u} is the displacement vector of a region of a crystal from its normal atomic positions. Therefore, the epitaxial strain of a gold dot which produces radially symmetric displacements, \mathbf{u} , should give rise to the light-dark contrast shown in cross section in Fig. 5 and observed in all the topographs. Note that the contrast goes to zero as $\mathbf{k} \cdot \mathbf{u}$ goes to zero and these points are used to locate the apparent surface in the transmitted-diffracted stereo pair.

Dislocation depths from asymmetrical Borrmann topographs

For the case of the two asymmetrical stereo topographs, the stereo direction (along which one observes a shift in image due to the change in direction of the exit X-ray beam) is along the diffracting planes and perpendicular to the projected directions of the diffracted and transmitted beams in the symmetrical case (Fig. 2). In this geometry, therefore, decoupling (or dechannelling) of the Bloch waves at or near the exit surface will not affect stereo depth measurements. Also, the gold dot images give a reliable indication of the location of the exit surface in this geometry, and the stereo shifts may be measured on either the $K\alpha_1$ or $K\alpha_2$ images.

The information about the position of the dislocation is transmitted along the diffracting planes in a Bloch wave until it is decoupled and exits from the crystal.

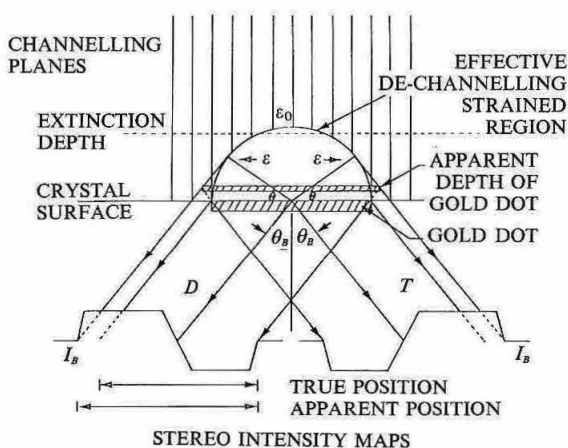


Fig. 5. Schematic drawing of Borrmann diffracted beam-transmitted beam stereo pair showing the apparent depth of the image of the gold dot due to a hemispherical strain field within the crystal around the gold dot. D is the diffracted beam, T is the transmitted beam, I is the background intensity, ϵ_0 is the effective dechannelling strain and ϵ shows the direction of strain to be radial outward from the center of the gold dot.

However, in this case the direction of the Bloch wave transmission is not along the normal to the crystal surface, but along paths at $\pm 10^\circ$ to this normal for the two topographs. Thus a stereo viewing angle of 20° is available in the topographs and no distortion or stereo shift corrections need to be made. This method, therefore, provides true stereo depth data on the dislocations in the crystal. The data of Table 1 show observed depths from very close to the exit surface ($3.5 \mu\text{m}$) through the entire thickness of the crystal ($270 \mu\text{m}$; less than 0.5% of the data were above $265 \mu\text{m}$) and supports the conjecture that these are the true depths of the dislocations in the crystal.

Dislocation depths from diffracted beam-transmitted beam Borrmann topographs

Table 1 gives the data for the observed depths of dislocations in the diffracted beam-transmitted beam method. Cottrell-Lomer dislocations and the dislocations grown-in or produced by scratching are listed separately. The Cottrell-Lomer dislocations are observed in the diffracted beam-transmitted beam method to cover a slightly narrower range of depths, but this range is shifted approximately $3 \mu\text{m}$ deeper into the crystal. As has been described above, the negative depths observed should be primarily due to the stereo imaging of the displacement field due to the gold dots, but the additional problem of stereo matching of the images of the gold dots could also affect the 'zero' of observations. The range of dislocation depths observed on an individual crystal, however, should only depend on the stereo imaging of the dislocations.

The small apparent stereo depths of the deepest dislocations indicates that the Borrmann Bloch wave is being decoupled into the diffracted and transmitted beams in the absence of a dislocation strain field at about $10 \mu\text{m}$ from the surface (a surprisingly large distance for surface relaxation effects). Without such a decoupling of the wave, the dislocations deep in the crystal would all appear at the one depth which marked the position of the surface with respect to the gold dots. True depths of these deeper dislocations, the Cottrell-Lomer and deep grown-in dislocations, are not obtained by this method. It is possible that the strain field from the gold dots is contributing to this decoupling of the Borrmann Bloch wave. Such an effect should produce apparent depths which change as the dislocation image approaches a gold dot and this is not observed.

Within the narrow region near the surface of the crystal, a Borrmann Bloch wave may be decoupled by dislocation strain to form the direct and diffracted beams which exit the crystal before they are strongly attenuated by kinematic absorption. The stereo information on the depth of these dislocations near the surface is carried out of the crystal in the two beams. Thus for dislocations near the exit surface of the crystal, the relative observed depths are equivalent to the relative true depths of the dislocations. The observed range of

depths, $18.2\ \mu\text{m}$, does correspond very well with the $18\ \mu\text{m}$ absorption depth through which this effect should occur.

Summary

The following conclusions are made from this study of the diffraction-transmission stereo pairs:

(1) The range of observed depths of the dislocations is comparable with $1/\mu$, where μ is the kinematic mass absorption coefficient in the crystal.

(2) The Borrmann Bloch wave is apparently separating into the diffracted and transmitted beams below the exit surface, not *at* the exit surface in nearly perfect crystal regions. This gives rise to a stereo effect in the images of 'deep' dislocations which makes them appear at a depth of approximately $1/\mu$. 'Shallow' dislocations (within $1/\mu$ of the surface) appear at their actual depths.

(3) The structure of the image of the gold dots supports the strain-image calculations of Kuriyama (1969) and Tanner (1976).

(4) A reliable method for accurately locating the exit surface in the stereo pair is needed. The uncertainty in surface location using the gold dots is approximately 3 to $5\ \mu\text{m}$ in the diffracted-transmitted pair and 1 to $3\ \mu\text{m}$ in the asymmetrical pair of stereo topographs.

The research was supported by the National Science Foundation and by a grant from the research office of

the Department of the Army. Dr Hamill wishes to express his thanks to the California Institute of Technology for research and teaching assistantships. The work of A. Illig on specimen preparation and photography is gratefully acknowledged.

References

- AZAROFF, L. V., KAPLOW, R., KATO, N., WEISS, R. J., WILSON, A. J. C. & YOUNG, R. A. (1974). *X-ray Diffraction*. New York: McGraw Hill.
- BOETTINGER, W. J., BURDETTE, H. E., KURIYAMA, M. & GREEN, R. E. JR (1976). *Rev. Sci. Instrum.* **47**, 906-911.
- BORRMANN, G. (1941). *Phys. Z.* **42**, 157-162.
- HARUTA, K. (1965). *J. Appl. Phys.* **36**, 1789-1790.
- JASSBY, K. M. & VREELAND, T. JR (1970). *Philos. Mag.* **21**, 1147-1168.
- KURIYAMA, M. (1969). *Acta Cryst.* **A25**, 682-693.
- KURIYAMA, M., EARLY, J. G. & BURDETTE, H. E. (1974). *J. Appl. Cryst.* **7**, 535-540.
- LANG, A. R. (1958). *J. Appl. Phys.* **29**, 597-598.
- LANG, A. R. (1959a). *J. Appl. Phys.* **30**, 1748-1755.
- LANG, A. R. (1959b). *Acta Cryst.* **12**, 249-250.
- NARASIMHAN, M. C. & ROESSLER, B. (1975). *Microstruct. Sci.* **3B**, 583-592.
- NARASIMHAN, M. C. & ROESSLER, B. (1976). Unpublished.
- TANNER, B. K. (1973). *J. Appl. Cryst.* **6**, 31-38.
- TANNER, B. K. (1976). *X-ray Diffraction Topography*. Oxford, New York, London: Pergamon Press.
- VREELAND, T. JR (1976). *J. Appl. Cryst.* **9**, 34-38.